



RESEARCH ARTICLE

10.1002/2015GC005904

Spatiotemporal variations of the slow slip event between 2008 and 2013 in the southcentral Alaska subduction zone

Yuning Fu¹, Zhen Liu¹, and Jeffrey T. Freymueller²¹Jet Propulsion Laboratory, California Institute of Technology, Pasadena, California, USA, ²Geophysical Institute, University of Alaska Fairbanks, Fairbanks, Alaska, USA

Key Points:

- The 2008–2013 SSE released most slip deficit accumulated in 2001–2008 steady period
- The 2008–2013 SSE shows both lateral and downdip propagation during this event
- Seismicity rate increased from 2009, coinciding with the SSE

Supporting Information:

- Supporting Information S1

Correspondence to:

Z. Liu,
zhen.liu@jpl.nasa.gov

Citation:

Fu, Y., Z. Liu, and J. T. Freymueller (2015), Spatiotemporal variations of the slow slip event between 2008 and 2013 in the southcentral Alaska subduction zone, *Geochem. Geophys. Geosyst.*, 16, doi:10.1002/2015GC005904.

Received 7 MAY 2015

Accepted 6 JUL 2015

Accepted article online 14 JUL 2015

Abstract We apply a Kalman filter-based time-dependent slip inversion method to model a long-term Slow Slip Event (SSE) in the southcentral Alaska subduction zone from 2008 to 2013. This event occurred downdip of the asperity that ruptured in the 1964 earthquake, the same part of plate interface that slipped during a previous SSE between 1998 and 2001. Most of the slip deficit that accumulated during the steady period between 2001 and 2008 (8 years total) in the SSE source region was released by this SSE. Our results indicate both lateral and downdip propagation during this event. The SSE started at the end of 2008 at the upper section of the slip patch, and gradually propagated to the east and to the deeper part of the interface. Our results indicate no connection between this SSE in Upper Cook Inlet and another SSE in Lower Cook Inlet that started in 2010. Analysis of the earthquake catalog in the southcentral Alaska subduction zone shows a clear increase in seismicity associated with the 2008–2013 SSE. With the data from a newly available continuous GPS site, we now can better constrain the start time of the 1998–2001 SSE as ~ 1998.58 .

1. Introduction

The discovery of Slow Slip Events (SSEs) complements the picture of crustal deformation at subduction zones during earthquake cycles. SSEs have been reported at most of the subduction zones with adequate geodetic measurements, although the durations of SSEs vary considerably ranging from days to years [e.g., Schwartz and Rokosky, 2007; Liu, 2014].

At the southcentral Alaska subduction zone, the underthrusting of the Pacific plate beneath the North American plate led to the Great 1964 Alaska earthquake ($M_w = 9.2$), the second largest earthquake ever recorded instrumentally [Kanamori, 1977]. Several SSEs have been discovered there since GPS measurement started in Alaska in 1993 (Figure 1). Ohta *et al.* [2006] identified a 3 year long-term SSE between 1998 and 2001 in Upper Cook Inlet. Wei *et al.* [2012] found another SSE between 2010 and 2011 in Lower Cook Inlet. Fu and Freymueller [2013] reported a new large SSE in Upper Cook Inlet starting from the end of 2008, and this event was still ongoing as the publication of Fu and Freymueller [2013]. This event finished in 2013 based on GPS measurement. It had a duration of more than 4 years, providing a unique opportunity for us to examine the temporal and spatial slip characteristics of the 2008–2013 SSE in the southcentral Alaska subduction zone.

In this study, we analyze the continuous GPS observations in the southcentral Alaska subduction zone, and investigate the spatiotemporal slip variations during the entire SSE between 2008 and 2013. This is the first long-term SSE in the Upper Cook Inlet of southcentral Alaska subduction zone for which we have a dense continuous GPS network coverage, unlike the earlier one that occurred in 1998–2001 [Ohta *et al.*, 2006]. Additionally, we also investigate if there was a connection between the SSE at Upper Cook Inlet and SSE in Lower Cook Inlet identified by Wei *et al.* [2012]. Finally, we analyze the earthquake catalog within the southcentral Alaska subduction zone to see if there is any evidence for seismicity increase associated with the SSE.

2. Continuous GPS Measurement

GPS measurements in Alaska started since ~ 1993 with repeated campaign mode surveys of sites in southern Alaska [Freymueller *et al.*, 2008]. A few continuous GPS stations existed in Alaska as early as 1996, but

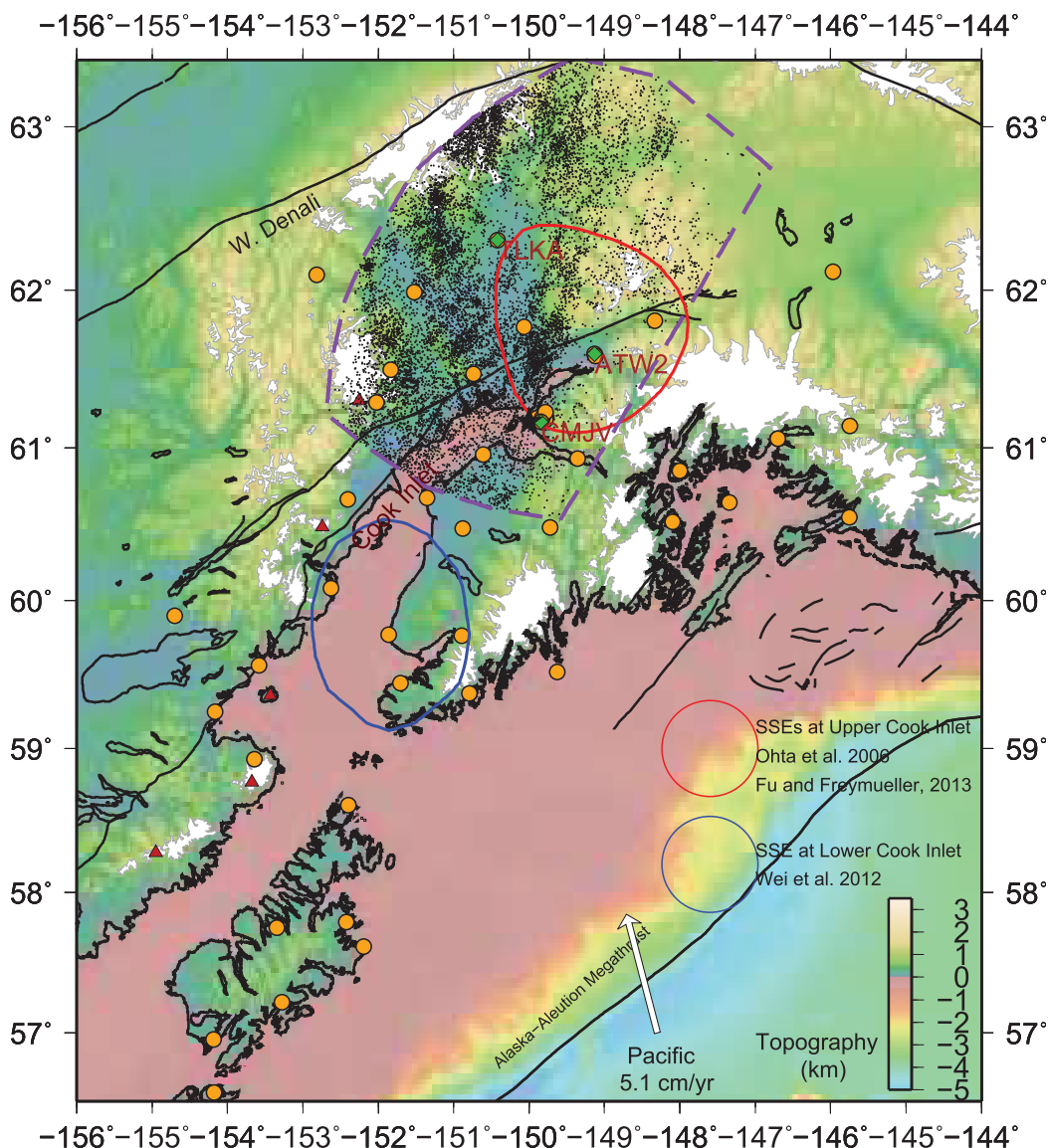


Figure 1. Distribution of continuous GPS stations (orange circles) used in this research. Red solid line indicates the location of SSEs at Upper Cook Inlet [Ohta et al., 2006; Fu and Freymueller, 2013]; blue solid line shows location of SSE at Lower Cook Inlet [Wei et al., 2012]. Purple dashed line circles the study region of seismicity rate change (Figure 7), and the black dots are earthquakes during the period of 2008–2013 SSE. The fault system in the southcentral Alaska subduction zones is outlined with black lines. Red triangles represent locations of volcanoes.

the number of stations remained small until the Plate Boundary Observatory (PBO) established an observational network in Alaska with a large number of continuous GPS stations between 2005 and 2008. In this study, we analyzed 45 continuous GPS stations located in the southcentral Alaska subduction zone. Thirty-three of them belong to the PBO network, and 12 of them are maintained by other institutes and organizations, such as the University of Alaska Fairbanks, the National Oceanic and Atmospheric Administration (NOAA), the U.S. Geological Survey (USGS), the Alaska Department of Transportation, the Federal Aviation Administration and local land surveyors. We chose stations that are far away from volcanoes and far enough from the Denali fault so they are not affected by volcanic deformation and the postseismic transients of the 2002 Denali earthquake. Figure 1 shows the distribution of continuous GPS stations used in this study.

All the GPS data were processed in point positioning mode [Zumberge et al., 1997] using GIPSY/OASIS software version goa-5.0 developed by the Jet Propulsion Laboratory (JPL). JPL’s reprocessed products for satellite orbits and clocks [Desai et al., 2011] were used. Absolute antenna phase center models for both satellite and receiver [Schmid et al., 2007] are adopted for correction. Ocean tidal loading is corrected with ocean

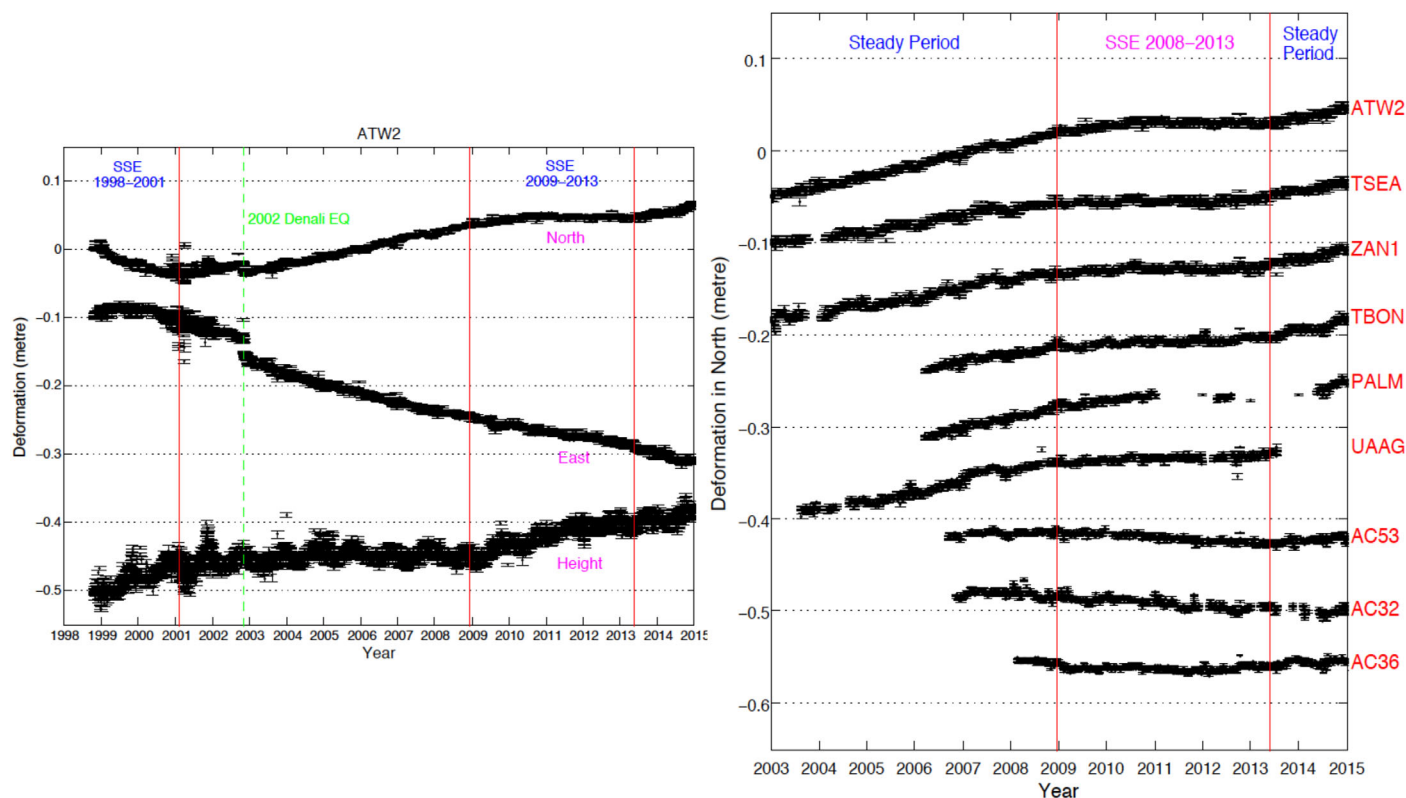


Figure 2. (left) Time series (relative to stable North America) of continuous GPS station ATW2 located at Palmer, Alaska. This is a combined time series between current PBO station ATW2 (from 2000 to now) and a previously existed collocated station ATWC (from 1998 to 2001). (right) North component of time series for typical continuous GPS stations showing the deformation history, relative to North American plate.

tide model TPX07.0 [Egbert and Erofeeva, 2002] and loading deformation is computed in a consistent reference frame (center of mass of Earth system) [Fu *et al.*, 2012a]. GPS daily solutions are then transformed into the ITRF2008 reference frame [Altamimi *et al.*, 2011]. More detailed GPS data processing information are given by Fu and Freymueller [2012].

In Figure 2, we plot the continuous GPS time series for station ATW2, located at Palmer, Alaska (61.598°N, 149.132°W). The series is relative to stable North American plate. This is a combined time series between current PBO station ATW2 (from October 2000 to now) and a previously existing collocated station ATWC (from 1998 to June 2001), applying a survey offset estimated from several months of overlap between the sites.

Two long-term SSEs in this part of the southcentral Alaska subduction zone have been recorded by GPS measurements since late 1990s. The first event occurred between 1998 and 2001 (Figure 2). Ohta *et al.* [2006] studied GPS measurements (most of them in campaign mode) for this event and investigated the cumulative displacements. They found that this SSE occurred downdip of an asperity that ruptured in the 1964 earthquake with cumulative slip >10 cm and equivalent moment magnitude of 7.2. Because Ohta *et al.* [2006] did not have continuous measurement for the early 1998, the event onset time was not well constrained, and this first event ended at early 2001. After ~ 8 years of steady interseismic period (2001–2008), the second event started at the end of 2008 (Figure 2). Fu and Freymueller [2013] analyzed GPS time series until the end of 2012 for the second event, and this second event was still ongoing when Fu and Freymueller [2013] was published. They divided the event into two phases according to different temporal slip variation features and calculated the accumulated displacements. They concluded that the second event occurred on the same part of the subduction interface as the earlier 1998–2001 event with moment magnitude of 7.5 until the end of 2012.

Figure 2 shows that the second SSE ended in 2013. Seasonal crustal oscillations, especially in the vertical direction, are significant in southern Alaska due to large hydrological (snow) loading effect [Fu *et al.*, 2012b].

The red lines indicating the SSE starting time and ending time are from parametric fits to the GPS time series. We fit each GPS time series with a linear trend and seasonal terms for interseismic period, and seasonal and logarithmic functions for the SSE period, and then adopt a grid search method to estimate the approximate timing of this event (the final estimation of the timing of the transient will be determined more accurately with our Kalman filter, see section 3.1). The duration of this SSE in Alaska is more than 4 years (~4.4 years from this GPS time series fit) and is much longer than most previously identified SSEs at other subduction zones along the Pacific Rim. Other identified SSE duration are 2–3 weeks in Cascadia [Dragert et al., 2001; Rogers and Dragert, 2003; Schmidt and Gao, 2010], ~6 months in Mexico [Kostoglodov et al., 2003; Larson et al., 2004], a wide range of SSEs in New Zealand: short-term ~10 days [Douglas et al., 2005], 7–270 days [Bartlow et al., 2014; Wallace and Eberhart-Phillips, 2013], and one and half year [Wallace and Beavan, 2006], and several months in Costa Rica [Jiang et al., 2012; Dixon et al., 2014], 2 months in central Japan [Ozawa et al., 2003], more than 2 years in Bungo Channel, southwest Japan [Hirose et al., 1999; Liu et al., 2010, 2015], and 5 years in Tokai [Ozawa et al., 2001; Yamamoto et al., 2005; Liu et al., 2010]. A recent study with fossil coral microatolls [Meltzner et al., 2015] identified a SSE as long as 15 years in the Banyak Islands, Sumatra.

3. Spatiotemporal Slip Variations

To investigate how the slip propagates with time during a SSE, time-dependent inversion filters and strategies have been applied to Cascadia [e.g., McGuire and Segall, 2003; McCaffrey, 2009; Bartlow et al., 2011], Japan [e.g., Miyazaki et al., 2006; Liu et al., 2010] and other subduction zone. However, no published paper has yet investigated the spatiotemporal slip variation of the Upper Cook Inlet SSEs. Since the continuous GPS network in Alaska has been greatly improved during the last decade thanks to the PBO project, detailed time-variable slip history can now be recovered.

3.1. Time-Dependent Inversion Strategy

In this study, we adopt a modified network inversion filter [Segall and Matthews, 1997; McGuire and Segall, 2003; Liu et al., 2010] to model the time-dependent slip variations of the second SSE starting at the end of 2008. The network inversion filter is based on a Kalman filter that distinguishes spatially correlated transient signals due to fault slips from noncorrelated local effects (e.g., random benchmark motion). GPS position time series can be modeled as a function of time t and site location x [Segall and Matthews, 1997].

$$u(x, t) = \int_A S_p(\xi, t) G_{pq}^f(x, \xi) n_q(\xi) dA(\xi) + Ff(t) + L(x, t) + \mathcal{E}(t) \quad (1)$$

The first component on the right side of equation (1) is the displacement (at time t) due to the slip (S_p) of subfault $A(\xi)$. G_{pq}^f is the Green's function due to slip in elastic half-space [Okada, 1985], n_q is the unit normal to the fault surface $A(\xi)$. The second term $Ff(t)$ represents reference frame error. The third term $L(x, t)$ is random benchmark motion. The last term $\mathcal{E}(t)$ is measurement error and is assumed to follow a normal distribution with zero mean and covariance $\sigma^2 \Sigma(t)$, where $\Sigma(t)$ is the covariance matrix of GPS positions and σ^2 is a scale factor to account for unmodeled errors in GPS data processing. Note that in (1) we assume that the position time series has been detrended (i.e., the inter-SSE velocity has been removed). This method has been applied successfully to model postseismic transients [e.g., Bürgmann et al., 2002], SSEs on the San Andreas Fault zone [e.g., Murray and Segall, 2005], in Japan [e.g., Liu et al., 2010, 2015] and Cascadia [e.g., Bartlow et al., 2011].

We adopt the Slab 1.0 model for the subduction interplate geometry [Hayes et al., 2012]. The subducting plate interface is reconstructed as a triangular mesh surface, and the elastostatic Green's functions G_{pq}^f are computed with triangular dislocation elements described by Jeyakumaran et al. [1992]. Spatial smoothing of the triangular mesh is based on the Fujiwara operator [Desbrun et al., 1999]. The typical mesh size is ~60 km. We conduct both spatial and temporal synthetic tests; please see supporting information Figure S1 for more information.

3.2. Modeling Results

Before inversion, we detrend the GPS time series based on the inter-SSE velocity estimated between 2005 and 2008.8, with the ending time chosen to be safely before the start time of the SSE (the start time is based

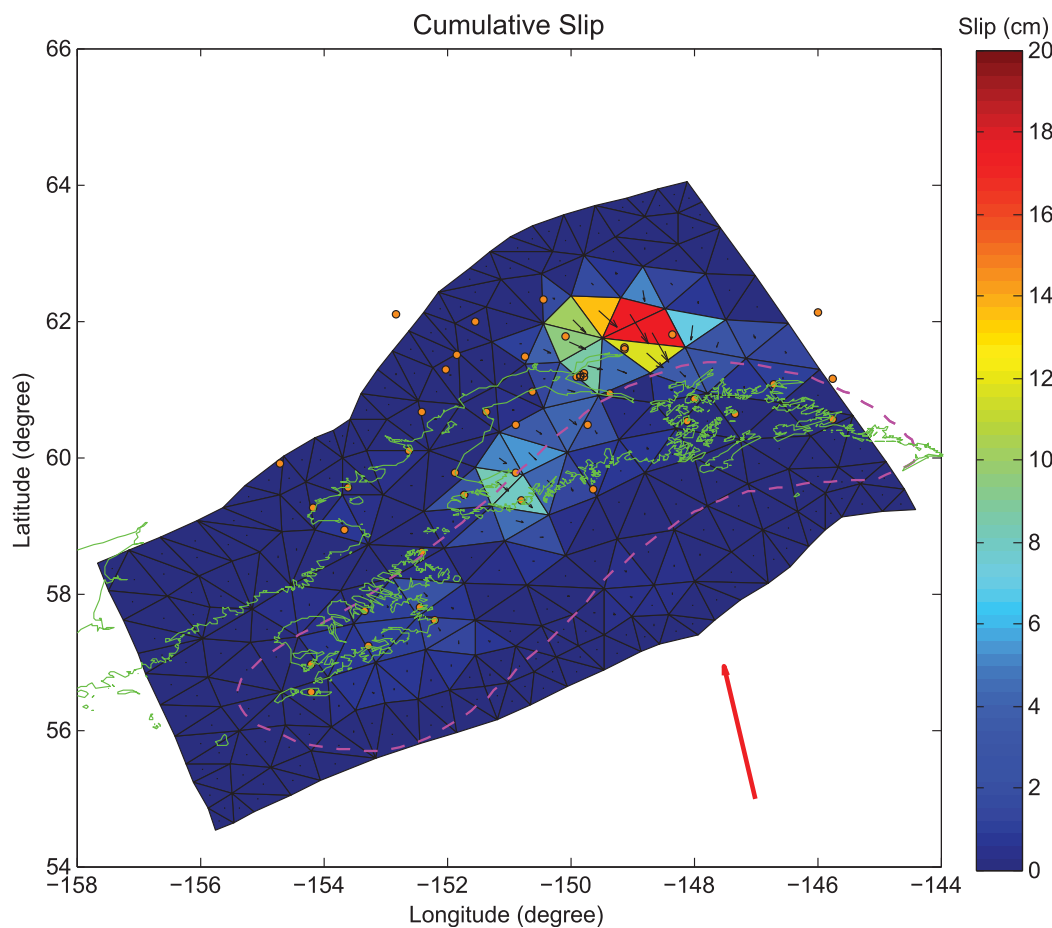


Figure 3. Cumulative slip for the SSE (2008.54–2013.89) inferred from our network filter inversion. The cumulative moment magnitude is ~ 7.6 . Magenta dashed line is the rupture area of the 1964 Alaska earthquake ($M_w = 9.2$). Orange circles indicate continuous GPS locations. Black arrows show the inverted cumulative slip amplitudes and directions. Red arrow indicates the Pacific-North America relative plate motion direction.

on the start of installation of the PBO). Subtracting this trend removes both the interseismic locking strain [Zweck *et al.*, 2002] and the postseismic deformation from the 1964 earthquake [Suito and Freymueller, 2009], and the residual deformations are only caused by the SSE transient event. Because displacements are estimated relative to the steady interseismic locking period, slip estimates reflect changes from the interseismic slip/locking distribution. In the Kalman filter inversion, we choose an a priori covariance with 1 sigma uncertainties of 2 mm/yr to account for potential uncertainties in the inter-SSE velocity estimates.

Figure 3 shows the cumulative slip in the SSE from our network filter inversion result, and Figure 4 plots the temporal slip variation of the SSE between 2008 and 2013, with a time interval of ~ 100 days. Figure 5 shows the comparisons between GPS positions and our modeling predictions. The event has a total moment magnitude of ~ 7.6 (assuming shear modulus = 50 GPa [Suito and Freymueller, 2009]). This event follows the scaling relationship that the released moment is proportional to the duration as suggested by Ide *et al.* [2007] which is distinct from regular earthquakes. In Figure 4, the magenta dashed line outlines the rupture area of the 1964 earthquake (M_w 9.2). Our results show that the SSE occurred downdip of the asperity that ruptured in the 1964 earthquake, at the same location of plate interface that slipped during the previous event between 1998 and 2001 [Ohta *et al.*, 2006]. Fu and Freymueller [2013] demonstrated that this part of the interface slips repeatedly in SSEs and releases its accumulated elastic strain; therefore, it does not build up a large slip deficit that will release in the next large earthquake.

We now can quantitatively estimate the slip budget for the regions of repeated SSEs. The total slip deficit during the ~ 8 years (2001–2008) steady period between two long-term SSEs is ~ 30 – 40 cm at shallow depth (coseismic earthquake rupture zone) and ~ 10 – 20 cm at downdip transitional zone (SSEs region)

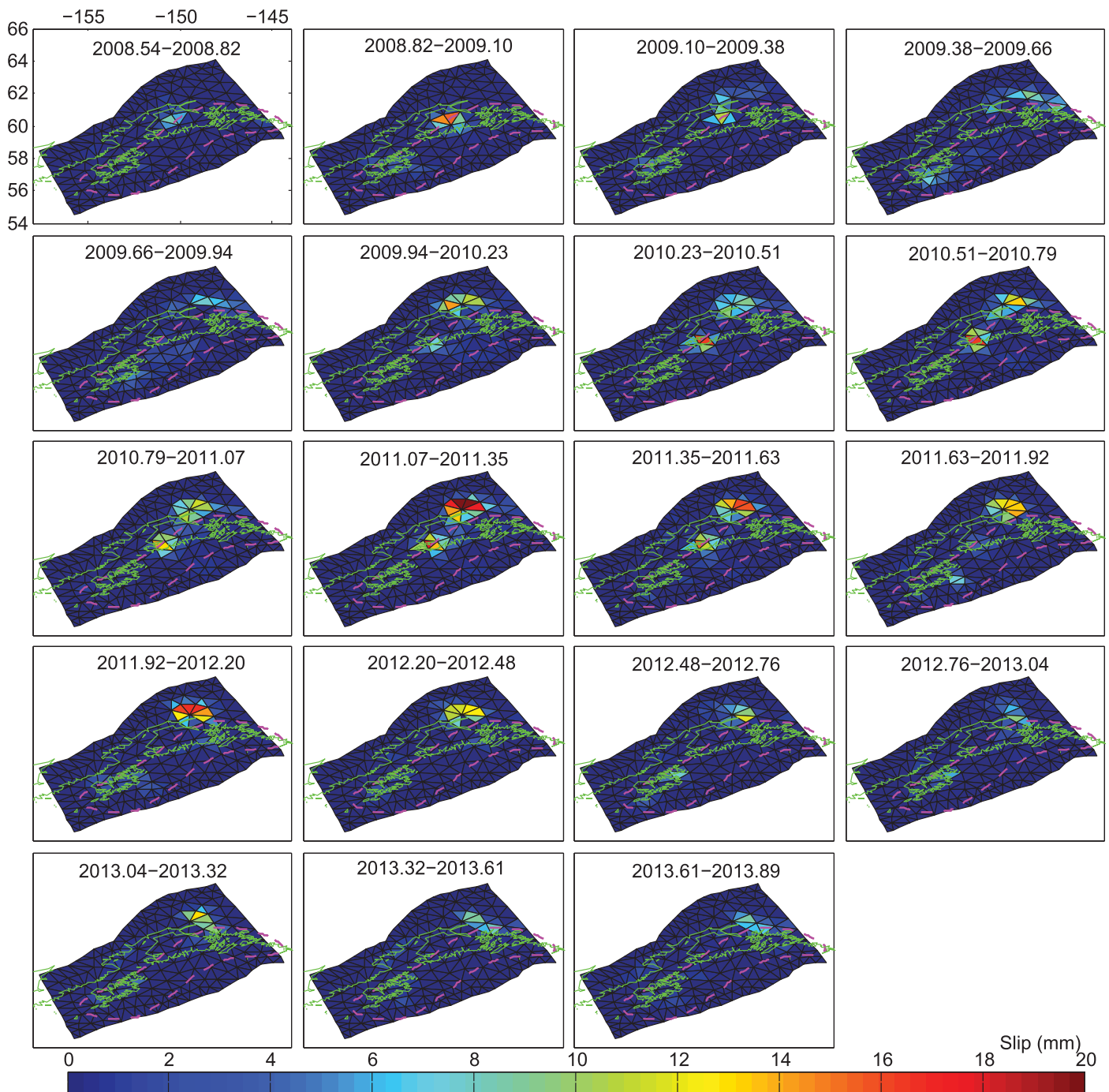


Figure 4. Spatiotemporal evolution of the SSE in the southcentral Alaska subduction zone between 2008 and 2013.

[Fu and Freymueller, 2013]. Our inversion result shows that ~ 10 – 20 cm cumulative slip has been released during the SSE (Figure 3). This suggests that nearly all the slip deficit accumulated over the steady 8 year period prior to the SSE has been released by aseismic transient slip in the SSE source region.

Our time-dependent inversion shows clear spatiotemporal slip variation (Figure 4). The slip initiated at the updip part of the SSE region after ~ 2008.82 . From 2009.1 to 2009.38, the slip gradually propagated from the upper section to the deeper portion, and then propagated laterally to the east from 2009.38 to 2009.66. Compared with the slip deficit (back slip or coupling) model for the inter-SSE period [Fu and Freymueller, 2013;

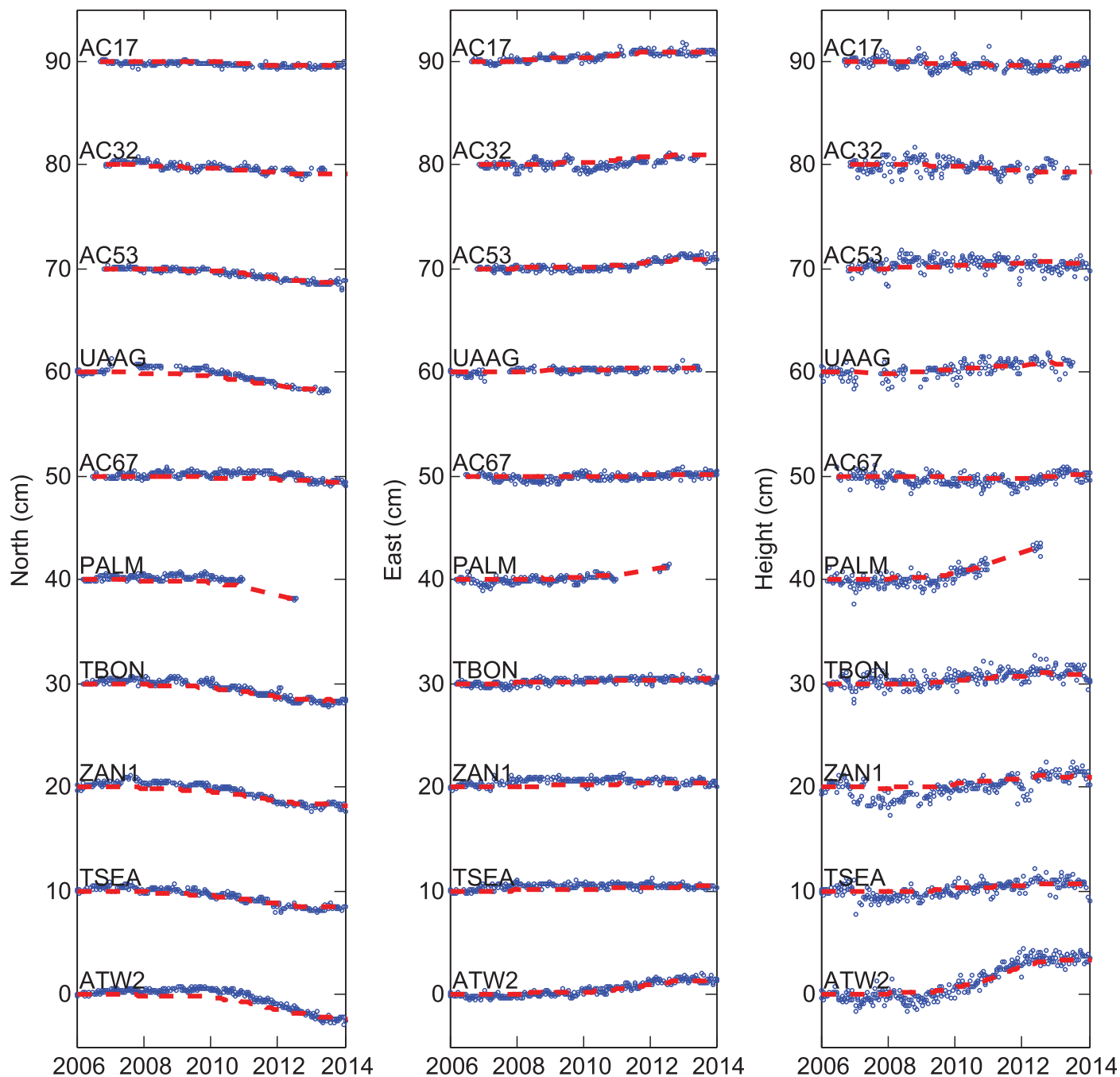


Figure 5. Comparison between GPS position time series and model predictions from 2006 to 2014. Blue dots are GPS measured crustal displacement, and red dashed lines are the model predictions from our slip inversion results.

Ohta *et al.*, 2006; Zweck *et al.*, 2002], the 2008–2013 event initiated in a less coupled location at the edge of the 1964 Prince William Sound asperity and then migrated laterally and down-dip into a more strongly locked region. The average migration speed is ~ 110 km/yr (~ 0.3 km/d), which is similar to what was observed for long-term slow slip transients in southwest Japan [Liu *et al.*, 2010] and SSE in Guerrero, Mexico [Radiguet *et al.*, 2011]. From 2010 to the end of the event, the slip remained in the deeper portion of the plate interface (Figure 4). Rate-and-state friction modeling suggests that the depth-dependent frictional properties can affect the SSE generation and propagation [Liu and Rice, 2005]. Similar lateral propagation of SSEs has been observed in other subduction zones, such as in Mexico [e.g., Radiguet *et al.*, 2011], and the Bungo Channel of southwest Japan [e.g., Liu *et al.*, 2010]. Along-dip migration of SSEs was identified at western Shikoku, Japan

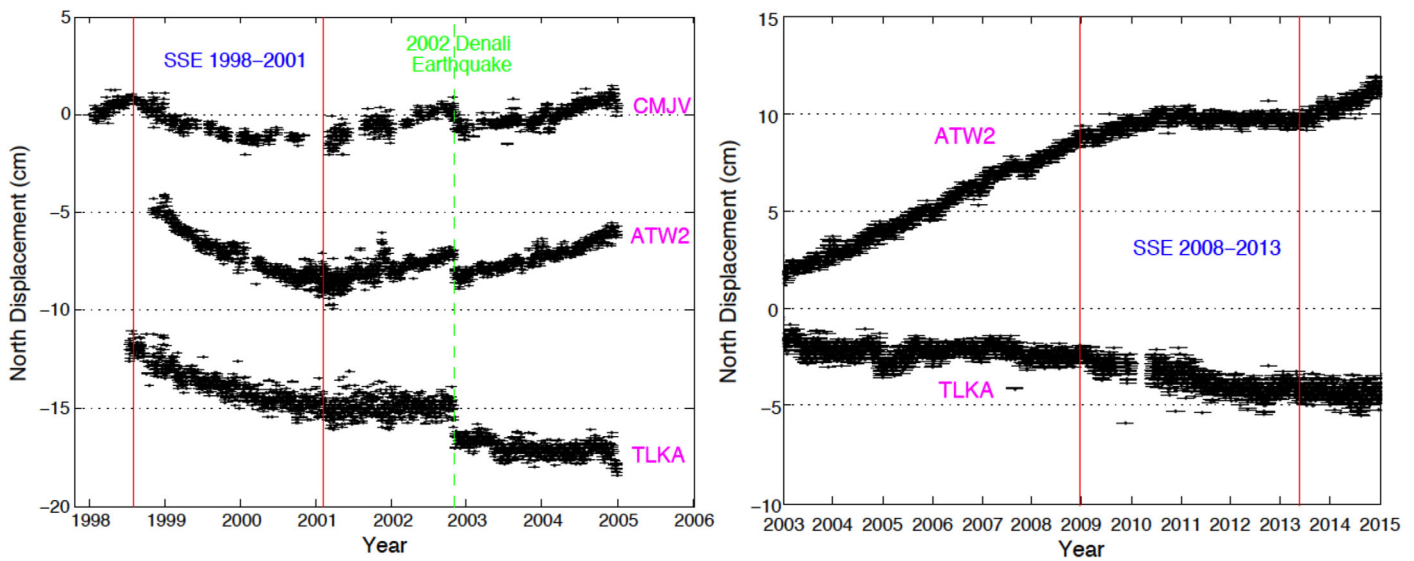


Figure 6. (left) North-component time series (relative to North America) of continuous GPS stations (CMJV, ATW2, and TLKA). CMJV indicates the 1998–2001 SSE started \sim 1998.58. The data for CMJV were not available when *Ohta et al.* [2006] was published. Red lines show the onset and ending times of the 1998–2001 SSE. Green dashed line shows the time of 2002 Denali earthquake. (right) North component of ATW2 and TLKA during the 2008–2013 SSE. CMJV did not have observations for this event.

[*Shelly et al.*, 2007a]. The SSE and tremor studies in Cascadia shows clear both lateral propagation and updip and downdip propagation of the SSEs [e.g., *Ghosh et al.*, 2009; *Wech and Bartlow*, 2014].

Besides the SSE in Upper Cook Inlet, our result also reveals a transient slip event in the Lower Cook Inlet from 2009.94 to 2011.63. This is part of the SSE reported by *Wei et al.* [2012]. Our results indicate there is no clear connection between SSEs in Upper Cook Inlet and Lower Cook Inlet, but instead there is a gap between them (Figure 4). The Lower Cook Inlet SSE started \sim 2009.94, and before that, there was no clear slip propagation movement from upper Cook Inlet southwestward to Lower Cook Inlet (Figure 4). The SSE in Lower Cook Inlet ended at \sim 2011.63 and lasted \sim 1.7 years, much shorter than the SSE in the Upper Cook Inlet (\sim 4.4 years). It appears to be an independent event.

3.3. Comparison With Previous 1998–2000 Event

Because of the limited continuous GPS stations (only three) that existed during the 1998–2001 event, we do not have enough continuous GPS measurements to perform a full time-dependent inversion. *Ohta et al.* [2006] studied the previous SSE mainly using annual campaign GPS observations, so the starting time of the previous event was not well constrained. Data from another continuous GPS station (CMJV) became available after the publication of *Ohta et al.* [2006]. CMJV was operated by a land surveying company and located at Anchorage Alaska (61.166°N, 149.845°W) with measurements as early as 1 January 1998. With those new data, we can now infer that the previous event started at \sim 1998.58 (Figure 6). The sharp bend in the CMJV time series indicates an abrupt onset of slip in this SSE, which is a much more abrupt onset than the later event.

Now we compare the continuous measurements for CMJV, ATW2, and TLKA (Talkeetna, Alaska; 62.308°N, 150.420°W), the only three continuous GPS sites that existed during the 1998–2001 SSE. Because these three stations are located at different distances relative to the trench (TLKA is at the north edge of the SSE region, ATW2 in the middle, and CMJV is at the south edge; see Figure 1), comparison of their time series may provide hints about the temporal slip evolution along the dip direction. Figure 6 (left) compares the north-component time series of the stations CMJV, ATW2, and TLKA during the 1998–2001 event. At the beginning of the event, both CMJV and TLKA show consistent southward movement with similar slope, which indicates that the 1998–2001 event might affect the entire SSE region from its beginning. Although ATW2 missed several months of measurements at the beginning of the 1998–2001 SSE, there was a clear difference in the velocity for the site ATW2 compared to CMJV and TLKA. We suggest two possibilities: the SSE source is localized at the central portion of the SSE region (close to ATW2), or there was a rapid propagation along dip for the 1998–2001 SSE. Unfortunately, the continuous GPS stations then were not dense

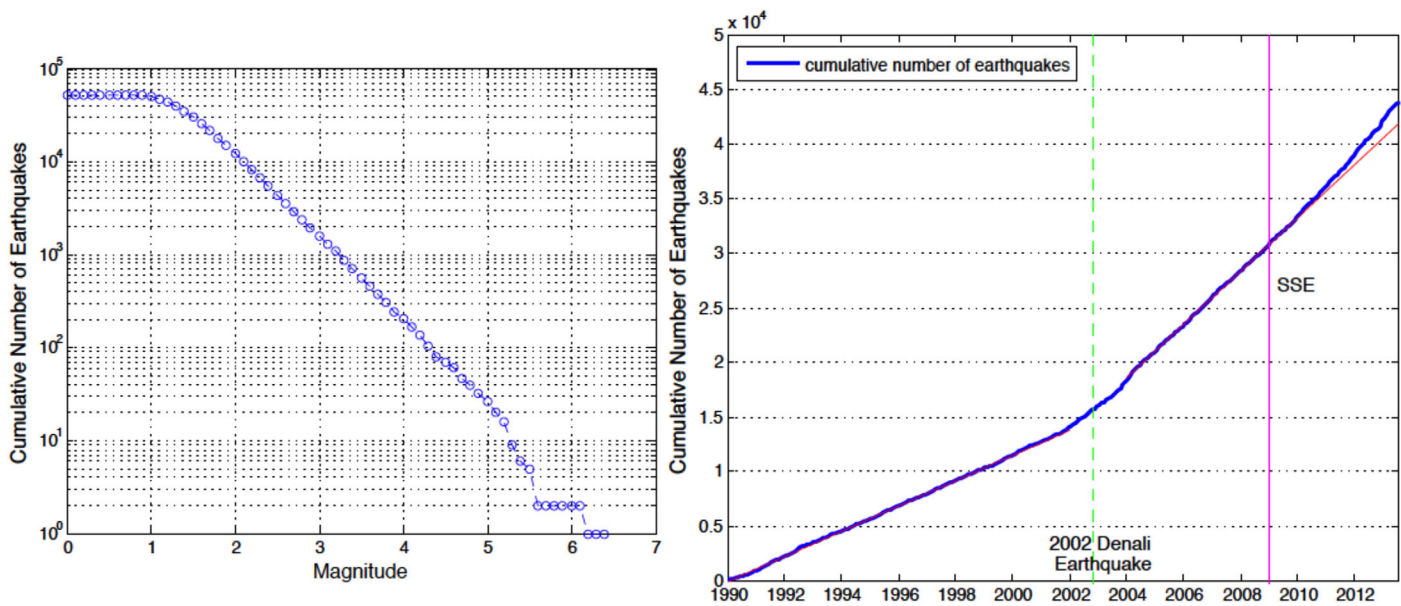


Figure 7. (left) Relationship between cumulative number of earthquakes and magnitude. (right) Cumulative number of earthquakes (Magnitude > 1.2) for the upper Cook Inlet region. The purple dashed line in Figure 1 indicates the study region. The seismicity rate significantly changed after the 2002 Denali $M_w = 7.9$ earthquake. It is also clear that the seismicity rate also increased since the beginning of the SSE that started from the end of 2008. The blue line shows the cumulative seismicity number from the ANSS earthquake catalog, and the red line is a linear fit for the periods between 1990 and 2002, and between 2004 and 2009, respectively.

enough to clarify these hypotheses. In Figure 6 (right), we also plot the north component of stations ATW2 and TLKA for the 2008–2013 event. CMJV did not have observations for this event. ATW2 also has a faster velocity rate than TLKA for the 2008–2013 event, as with the 1998–2001 event. A comparison of GPS series indicates that the slip rate of the 1998–2001 event was faster than that of the 2008–2013 event.

4. Seismicity Rate Change

Seismicity changes associated with SSEs have been found in a number of subduction zones and volcanic regions, such as Cascadia [Rogers and Dragert, 2003], the Boso Peninsula, Japan [Llenos et al., 2009; Hirose et al., 2014], Lower Cook Inlet Alaska [Wei et al., 2012], New Zealand [Bartlow et al., 2014], and Kilauea volcano [Segall et al., 2006]. To investigate the relationship between the SSE and seismicity rate change in the Upper Cook Inlet of southcentral Alaska Subduction zone, we analyze the earthquake catalog of the Advanced National Seismic System (ANSS) (<http://quake.geo.berkeley.edu/cnss/>). The original source for the Alaska region in the ANSS catalog is from the Alaska Earthquake Center (AEC). The purple dashed line in Figure 1 outlines our seismicity study area. We examine the seismicity records back to 1990. Figure 7 (left) shows the cumulative earthquake numbers versus magnitude, which indicates that the earthquake catalog is not complete for events with magnitude < 1.2. Therefore, in Figure 7 (right), we plot the cumulative number of earthquakes (Magnitude > 1.2) from 1990 to 2013.5 within the southcentral Alaska subduction zone. Because we are only interested in the seismicity along the subduction plate interface within the SSE region, we do not include earthquake with depths shallower than 30 km in order to exclude seismicity due to volcano activities and other surface faulting activity. In supporting information (Figure S2), we also show the results for earthquakes at all depths of this segment of the subduction zone.

On 3 November 2002, an $M_w = 7.9$ earthquake occurred at the Denali National Park, interior of Alaska. The cumulative earthquake plot (Figure 7, right) shows a clear seismicity rate change after the Denali $M_w = 7.9$ earthquake. In addition, around the onset time of the SSE analyzed in the study (the end of 2008 and early 2009), the seismicity rate also clearly increased relative to its pre-transient background level. In Figure 7 (right), the blue line shows the cumulative number of earthquakes from the ANSS earthquake catalog, and the red line is a linear fit for the period (2004–2009) prior to the SSE. In Figure 1, we also plot the earthquake locations within Upper Cook Inlet (purple dashed line) during the 2008–2013 SSE. Most of the seismicity occurred downdip of the SSE region. Since the region downdip of the SSE is where the larger stress increase

is expected, the dominant downdip concentration of earthquake clusters is consistent with the view that stress change due to SSE promotes earthquake occurrence. In Lower Cook Inlet, *Wei et al.* [2012] also detected a seismicity rate increase in mid-2010 associated with the SSE there.

5. Discussion

Low-frequency earthquakes or nonvolcanic tremor usually accompany SSEs [e.g., *Rogers and Dragert*, 2003; *Shelly et al.*, 2007b; *Liu et al.*, 2010; *Peng and Gomberg*, 2010]. Nonvolcanic tremors were suggested to be associated with fluid-rich conditions and have been attributed to fluid-induced shear slip along the plate interface [e.g., *Peng and Gomberg*, 2010; *Shelly et al.*, 2007b]. Although nonvolcanic tremor had been identified in southcentral Alaska subduction zone during the previous 1998–2001 event [*Peterson and Christensen*, 2009], as this manuscript was prepared, no published study has reported identified tremors on the plate interface beneath the upper Cook Inlet region during the recent SSE period (2008–2013). We hope further study can investigate the seismic data to determine if there were nonvolcanic tremors associated with the 2008–2013 SSE and any implication toward fluid condition of SSE source region.

Slow slip events have been observed globally at many subduction zones. They have been found both downdip and updip of the seismic rupture zone, releasing accumulated interseismic strain. The SSEs may precede and possibly trigger large earthquakes such as the great 2011 *Mw* 9.0 Tohoku-Oki earthquake [*Ozawa et al.*, 2012; *Vallée et al.*, 2013]. *Dixon et al.* [2014] studied SSEs at the Costa Rica Subduction zone and doubted the SSE's practical predictive capability for the timing of megathrust earthquakes. Here at southcentral Alaska subduction zone, SSEs repeatedly occur downdip of the coseismic rupture zone. No shallow slow slip has been identified, which may reflect the limitation of onshore GPS network. Our calculation of slip deficit budget indicates the SSE released most of the accumulated slip at that part of the interface. The SSE area did not experience significant slip during the 1964 earthquake [*Suito and Freymueller*, 2009]. Given the average coseismic rupture of ~20–25 m in the *Mw* 9.2 1964 earthquake, it may take ~400–500 years to build up elastic strain to another magnitude ~9 earthquake. In this regard, quantifying the aseismic versus seismic energy budget can provide crucial information in assessing the rupture limits and location, magnitude, and potential hazard of future great megathrust shocks [*Dixon et al.*, 2014; *Avouac*, 2015].

6. Conclusions

Our time-dependent slip inversion of the 2008–2013 SSE in the southcentral Alaska subduction zone shows that slip mainly occurred downdip of the asperity that ruptured in the 1964 earthquake, the same part of the plate interface that slipped during the previous event between 1998 and 2001. Most of the slip deficit that was accumulated during the steady interseismic period between 2001 and 2008 in the SSE source region was released by this long-term aseismic slow slip event. Our results show that this SSE started from the end of 2008 at the upper section of the SSE region and then gradually propagated laterally to the east and into the deeper part of plate interface. There is no clear connection between the 2008–2013 SSE in the Upper Cook Inlet and another SSE in the Lower Cook Inlet that started in 2010. Seismicity analysis based on regional earthquake catalog shows an increase in seismicity rate that coincides with the transient slip activity starting at the end of 2008. With newly available (historical) data from a continuous GPS site, we now provide better constraint on the onset time of the 1998–2001 event, and show that it had an abrupt onset that was very different from the start of the more recent event. The 1998–2001 event also had a faster slip rate in general.

References

- Altamimi, Z., X. Collilieux, and L. Métivier (2011), ITRF2008: An improved solution of the International Terrestrial Reference Frame, *J. Geod.*, *85*(8), 457–473, doi:10.1007/s00190-011-0444-4.
- Avouac, J.-P. (2015), From geodetic imaging of seismic and aseismic fault slip to dynamic modeling of the seismic cycle, *Annu. Rev. Earth Planet. Sci.*, *43*, 8.1–8.39, doi:10.1146/annurev-earth-060614-105302.
- Bartlow, N. M., S. Miyazaki, A. M. Bradley, and P. Segall (2011), Space-time correlation of slip and tremor during the 2009 Cascadia slow slip event, *Geophys. Res. Lett.*, *38*, L18309, doi:10.1029/2011GL048714.

Acknowledgments

The authors thank UNAVCO for maintaining the PBO GPS network in Alaska as part of the NSF EarthScope program. We appreciate Susan Owen for helpful discussions. The comments from two anonymous reviewers significantly improved the manuscript. We thank Jim Mitchell of Crazy Mountains Joint Venture for providing the CMJV data. All the data and results derived in the study are available from the authors. Y.F. was partly supported by the NASA Postdoctoral Program at Jet Propulsion Laboratory. J.T.F. was supported by NSF grant EAR12-15933. The research by Y.F. and Z.L. described in this paper was carried out at the Jet Propulsion Laboratory, California Institute of Technology, under a contract with the National Aeronautics and Space Administration (NASA).

- Bartlow, N. M., L. M. Wallace, R. J. Beavan, S. Bannister, and P. Segall (2014), Time-dependent modeling of slow slip events and associated seismicity and tremor at the Hikurangi subduction zone, New Zealand, *J. Geophys. Res. Solid Earth*, *119*, 734–753, doi:10.1002/2013JB010609.
- Bürgmann, R., S. Ergintav, P. Segall, E. H. Hearn, S. McClusky, R. E. Reilinger, H. Woith, and J. Zschau (2002), Time-dependent distributed afterslip on and deep below the Izmit earthquake rupture, *Bull. Seismol. Soc. Am.*, *92*, 126–137.
- Desai, S. D., W. Bertiger, B. Haines, N. Harvey, C. Sella, A. Sibthorpe, and J. P. Weiss (2011), Results from the reanalysis of global GPS data in the IGS08 reference frame, Abstract G53B-0904 presented at 2011 Fall Meeting, AGU, San Francisco, Calif., 5–9 Dec.
- Desbrun, M., M. Meyer, P. Schröder, and A. H. Barr (1999), Implicit fairing of irregular meshes using diffusion and curvature flow, in *Proceedings of the 26th Annual International Conference on Computer Graphics and Interactive Techniques*, pp. 317–324, ACM Press, N. Y., doi:10.1145/311535.311576.
- Dixon, T. H., Y. Jiang, R. Malservisi, R. McCaffrey, N. Voss, M. Protti, and V. Gonzalez (2014), Earthquake and tsunami forecasts: Relation of slow slip events to subsequent earthquake rupture, *Proc. Natl. Acad. Sci. U. S. A.*, *111*(48), 17,039–17,044, doi:10.1073/pnas.1412299111.
- Douglas, A., J. Beavan, L. Wallace, and J. Townend (2005), Slow slip on the northern Hikurangi subduction interface, New Zealand, *Geophys. Res. Lett.*, *32*, L16305, doi:10.1029/2005GL023607.
- Dragert, H., K. Wang, and T. S. James (2001), A silent slip event on the deeper Cascadia subduction interface, *Science*, *292*, 1525–1528.
- Egbert, G. D., and L. Erofeeva (2002), Efficient inverse modeling of barotropic ocean tides, *J. Atmos. Oceanic Technol.*, *19*, 183–204.
- Freymueller, J. T., H. Woodard, S. Cohen, R. Cross, J. Elliott, C. Larsen, S. Hreinsdottir, and C. Zweck (2008), Active deformation processes in Alaska, based on 15 years of GPS measurements, in *Active Tectonics and Seismic Potential of Alaska*, *Geophys. Monogr. Ser.*, vol. 179, edited by J. T. Freymueller et al., pp. 1–42, AGU, Washington, D. C., doi:10.1029/179GM02.
- Fu, Y., and J. T. Freymueller (2012), Seasonal and long-term vertical deformation in the Nepal Himalaya constrained by GPS and GRACE measurements, *J. Geophys. Res.*, *117*, B03407, doi:10.1029/2011JB008925.
- Fu, Y., and J. T. Freymueller (2013), Repeated large slow slip events at the south central Alaska Subduction zone, *Earth Planet. Sci. Lett.*, *375*, 303–311, doi:10.1016/j.epsl.2013.05.049.
- Fu, Y., J. T. Freymueller, and T. van Dam (2012a), The effect of using inconsistent ocean tidal loading models on GPS coordinate solutions, *J. Geod.*, *86*(6), 409–421, doi:10.1007/s00190-011-0528-1.
- Fu, Y., J. T. Freymueller, and T. Jensen (2012b), Seasonal hydrological loading in southern Alaska observed by GPS and GRACE, *Geophys. Res. Lett.*, *39*, L15310, doi:10.1029/2012GL052453.
- Ghosh, A., J. E. Vidale, J. R. Sweet, K. C. Creager, and A. G. Wech (2009), Tremor patches in Cascadia revealed by seismic array analysis, *Geophys. Res. Lett.*, *36*, L17316, doi:10.1029/2009GL039080.
- Hayes, G. P., D. J. Wald, and R. L. Johnson (2012), Slab1.0: A three-dimensional model of global subduction zone geometries, *J. Geophys. Res.*, *117*, B01302, doi:10.1029/2011JB008524.
- Hirose, H., K. Hirahara, F. Kimata, N. Fujii, and S. Miyazaki (1999), A slow thrust slip event following the two 1996 Hyuganada earthquakes beneath the Bungo Channel, southwest Japan, *Geophys. Res. Lett.*, *26*, 3237–3240.
- Hirose, H., T. Matsuzawa, T. Kimura, and H. Kimura (2014), The Boso slow slip events in 2007 and 2011 as a driving process for the accompanying earthquake swarm, *Geophys. Res. Lett.*, *41*, 2778–2785, doi:10.1002/2014GL059791.
- Ide, S., G. C. Beroza, D. R. Shelly, and T. Uchide (2007), A scaling law for slow earthquakes, *Nature*, *447*, 76–79, doi:10.1038/nature05780.
- Jeyakumaran, M., J. W. Rudnicki, and L. M. Keer (1992), Modeling slip zones with triangular dislocation elements, *Bull. Seismol. Soc. Am.*, *83*(5), 2153–2169.
- Jiang, Y., S. Wdowinski, T. H. Dixon, M. Hackl, M. Protti, and V. Gonzalez (2012), Slow slip events in Costa Rica detected by continuous GPS observations, 2002–2011, *Geochem. Geophys. Geosyst.*, *13*, Q04006, doi:10.1029/2012GC004058.
- Kanamori, H. (1977), The energy release of great earthquakes, *J. Geophys. Res.*, *82*, 2981–2987.
- Kostoglodov, V., S. K. Singh, J. A. Santiago, S. I. Franco, K. M. Larson, A. R. Lowry, and R. Bilham (2003), A large silent earthquake in the Guerrero seismic gap, Mexico, *Geophys. Res. Lett.*, *30*(15), 1807, doi:10.1029/2003GL017219.
- Larson, K. M., A. R. Lowry, V. Kostoglodov, W. Hutton, O. Sánchez, K. Hudnut, and G. Suárez (2004), Crustal deformation measurements in Guerrero, Mexico, *J. Geophys. Res.*, *109*, B04409, doi:10.1029/2003JB002843.
- Liu, Y. (2014), Source scaling relations and along-strike segmentation of slow slip events in a 3-D subduction fault model, *J. Geophys. Res. Solid Earth*, *119*, 6512–6533, doi:10.1002/2014JB011144.
- Liu, Y., and J. R. Rice (2005), Aseismic slip transients emerge spontaneously in three-dimensional rate and state modeling of subduction earthquake sequences, *J. Geophys. Res.*, *110*, B08307, doi:10.1029/2004JB003424.
- Liu, Z., S. Owen, D. Dong, P. Lundgren, F. Webb, E. Hetland, and M. Simons (2010), Integration of transient strain events with models of plate coupling and areas of great earthquakes in southwest Japan, *Geophys. J. Int.*, *181*, 1292–1312, doi:10.1111/j.1365-246X.2010.04599.x.
- Liu, Z., A. Moore, and S. Owen (2015), Recurrent slow slip event reveals the interaction with seismic slow earthquakes and disruption from large earthquake, *Geophys. J. Int.*, *202*(3), 1555–1565, doi:10.1093/gji/ggv238.
- Llenos, A. L., J. J. McGuire, and Y. Ogata (2009), Modeling seismic swarms triggered by aseismic transients, *Earth Planet. Sci. Lett.*, *281*, 59–69.
- McCaffrey, R. (2009), Time-dependent inversion of three-component continuous GPS for steady and transient sources in northern Cascadia, *Geophys. Res. Lett.*, *36*, L07304, doi:10.1029/2008GL036784.
- McGuire, J. J., and P. Segall (2003), Imaging of aseismic slip transients recorded by dense geodetic networks, *Geophys. J. Int.*, *155*, 778–788, doi:10.1111/j.1365-246X.2003.02022.x.
- Meltzner, A. J., et al. (2015), Time-varying interseismic strain rates and similar seismic ruptures on the Nias–Simeulue patch of the Sunda megathrust, *Quat. Sci. Rev.*, *122*, 258–281, doi:10.1016/j.quascirev.2015.06.003.
- Miyazaki, S., P. Segall, J. J. McGuire, T. Kato, and Y. Hatanaka (2006), Spatial and temporal evolution of stress and slip rate during the 2000 Tokai slow earthquake, *J. Geophys. Res.*, *111*, B03409, doi:10.1029/2004JB003426.
- Murray, J. R., and P. Segall (2005), Spatio-temporal evolution of a transient slip event on the San Andreas fault near Parkfield, California, *J. Geophys. Res.*, *110*, B09407, doi:10.1029/2005JB003651.
- Ohta, Y., J. Freymueller, S. Hreinsdottir, and H. Suito (2006), A large slow slip event and the depth of the seismogenic zone in the south central Alaska subduction zone, *Earth Planet. Sci. Lett.*, *247*(1–2), 108–116, doi:10.1016/j.epsl.2006.05.013.
- Okada, Y. (1985), Surface deformation due to shear and tensile faults in a halfspace, *Bull. Seismol. Soc. Am.*, *75*(4), 1135–1154.
- Ozawa, S., M. Murakami, and T. Tada (2001), Time-dependent inversion study of the slow thrust event in the Nankai Trough subduction zone, southwestern Japan, *J. Geophys. Res.*, *106*, 787–802.
- Ozawa, S., S. Miyazaki, Y. Hatanaka, T. Imakiire, M. Kaidzu, and M. Murakami (2003), Characteristic silent earthquakes in the eastern part of the Boso Peninsula, central Japan, *Geophys. Res. Lett.*, *30*(6), 1283, doi:10.1029/2002GL016665.

- Ozawa, S., T. Nishimura, H. Munekane, H. Suito, T. Kobayashi, M. Tobita, and T. Imakiire (2012), Preceding, coseismic, and postseismic slips of the 2011 Tohoku earthquake, Japan, *J. Geophys. Res.*, *117*, B07404, doi:10.1029/2011JB009120.
- Peng, Z., and J. Gombert (2010), An integrated perspective of the continuum between earthquakes and slow-slip phenomena, *Nat. Geosci.*, *3*, 599–607, doi:10.1038/ngeo940.
- Peterson, C. L., and D. H. Christensen (2009), Possible relationship between nonvolcanic tremor and the 1998–2001 slow slip event, south central Alaska, *J. Geophys. Res.*, *114*, B06302, doi:10.1029/2008JB006096.
- Radiguet, M., F. Cotton, M. Vergnolle, M. Campillo, B. Valette, V. Kostoglodov, and N. Cotte (2011), Spatial and temporal evolution of a long term slow slip event, the 2006 Guerrero slow slip event, *Geophys. J. Int.*, *184*(2), 816–828, doi:10.1111/j.1365-246X.2010.04866.x.
- Rogers, G., and H. Dragert (2003), Episodic tremor and slip on the Casca-dia subduction zone: The chatter of silent slip, *Science*, *300*, 1942–1943, doi:10.1126/science.1084783.
- Schmid, R., P. Steigenberger, G. Gendt, M. Ge, and M. Rothacher (2007), Generation of a consistent absolute phase center correction model for GPS receiver and satellite antennas, *J. Geod.*, *81*, 781–798, doi:10.1007/s00190-007-0148-y.
- Schmidt, D. A., and H. Gao (2010), Source parameters and time-dependent slip distributions of slow slip events on the Cascadia subduction zone from 1998 to 2008, *J. Geophys. Res.*, *115*, B00A18, doi:10.1029/2008JB006045.
- Schwartz, S. Y., and J. M. Rokosky (2007), Slow slip events and seismic tremor at circum-Pacific subduction zones, *Rev. Geophys.*, *45*, RG3004, doi:10.1029/2006RG000208.
- Segall, P., and M. Matthews (1997), Time dependent inversion of geodetic data, *J. Geophys. Res.*, *102*, 22,391–22,410.
- Segall, P., E. Desmarais, D. Shelly, A. Miklius, and P. Cervelli (2006), Earthquakes triggered by silent slip events on Kilauea Volcano, Hawaii, *Nature*, *442*, 71–74, doi:10.1038/nature04938.
- Shelly, D. R., G. C. Beroza, and S. Ide (2007a), Complex evolution of transient slip derived from precise tremor locations in western Shikoku, Japan, *Geochem. Geophys. Geosyst.*, *8*, Q10014, doi:10.1029/2007GC001640.
- Shelly, D. R., G. C. Beroza, and S. Ide (2007b), Non-volcanic tremor and low-frequency earthquake swarms, *Nature*, *446*, 305–307, doi:10.1038/nature05666.
- Suito, H., and J. T. Freymueller (2009), A viscoelastic and afterslip postseismic deformation model for the 1964 Alaska earthquake, *J. Geophys. Res.*, *114*, B11404, doi:10.1029/2008JB005954.
- Vallée, M., et al. (2013), Intense interface seismicity triggered by a shallow slow slip event in the Central Ecuador subduction zone, *J. Geophys. Res. Solid Earth*, *118*, 2965–2981, doi:10.1002/jgrb.50216.
- Wallace, L. M., and J. Beavan (2006), A large slow slip event on the central Hikurangi subduction interface beneath the Manawatu region, North Island, New Zealand, *Geophys. Res. Lett.*, *33*, L11301, doi:10.1029/2006GL026009.
- Wallace, L. M., and D. Eberhart-Phillips (2013), Newly observed, deep slow slip events at the central Hikurangi margin, New Zealand: Implications for downdip variability of slow slip and tremor, and relationship to seismic structure, *Geophys. Res. Lett.*, *40*, 5393–5398, doi:10.1002/2013GL057682.
- Wech, A. G., and N. M. Bartlow (2014), Slip rate and tremor genesis in Cascadia, *Geophys. Res. Lett.*, *41*, 392–398, doi:10.1002/2013GL058607.
- Wei, M., J. J. McGuire, and E. Richardson (2012), A slow slip event in the south central Alaska Subduction Zone and related seismicity anomaly, *Geophys. Res. Lett.*, *39*, L15309, doi:10.1029/2012GL052351.
- Yamamoto, E., S. Matsumura, and T. Ohkubo (2005), A slow slip event in the Tokai area detected by tilt and seismic observation and its possible recurrence, *Earth Planets Space*, *57*, 917–923.
- Zumberge, J. F., M. B. Heflin, D. C. Jefferson, M. M. Watkins, and J. F. H. Webb (1997), Precise point positioning for the efficient and robust analysis of GPS data from large networks, *J. Geophys. Res.*, *102*, 5005–5017, doi:10.1029/96JB03860.
- Zweck, C., J. T. Freymueller, and S. C. Cohen (2002), Three-dimensional elastic dislocation model of the post-seismic response to the 1964 Alaska earthquake, *J. Geophys. Res.*, *107*(B4), doi:10.1029/2001JB000409.